

# Synaptotagmin 7 splice variants differentially regulate synaptic vesicle recycling

Tuhin Virmani<sup>1</sup>, Weiping Han<sup>1,2</sup>,  
Xinran Liu<sup>1,3</sup>, Thomas C. Südhof<sup>1,2,3</sup> and  
Ege T. Kavalali<sup>1,4,5</sup>

<sup>1</sup>Center for Basic Neuroscience, Departments of <sup>3</sup>Molecular Genetics and <sup>4</sup>Physiology and <sup>2</sup>Howard Hughes Medical Institute, The University of Texas Southwestern Medical Center, Dallas, TX 75390-9111, USA

<sup>5</sup>Corresponding author  
e-mail: Ege.Kavalali@UTSouthwestern.edu

**The speed of synaptic vesicle recycling determines the efficacy of neurotransmission during repetitive stimulation. Synaptotagmins are synaptic C<sub>2</sub>-domain proteins that are involved in exocytosis, but have also been linked to endocytosis. We now demonstrate that upon expression in transfected neurons, a short splice variant of synaptotagmin 7 that lacks C<sub>2</sub>-domains accelerates endocytic recycling of synaptic vesicles, whereas a longer splice variant that contains C<sub>2</sub>-domains decelerates recycling. These results suggest that alternative splicing of synaptotagmin 7 acts as a molecular switch, which targets vesicles to fast and slow recycling pathways.**

**Keywords:** FM1-43/hippocampal synapse/kiss and run/ synaptic vesicle recycling/synaptotagmin 7

## Introduction

At the synapse, Ca<sup>2+</sup>-triggered synaptic vesicle exocytosis is followed by synaptic vesicle endocytosis and recycling. At least two recycling pathways for synaptic vesicles exist: a slow pathway whereby empty vesicles are endocytosed via clathrin-coated pits and may pass through an endosomal intermediate (Heuser and Reese, 1973; Betz and Bewick, 1993; Liu and Tsien, 1995; Koenig and Ikeda, 1996; Takei *et al.*, 1996; Richards *et al.*, 2000) and a fast pathway (occasionally referred to as ‘kiss and run’ or ‘kiss and stay’ to account for the retention of synaptic vesicles at the active zone during recycling) whereby empty vesicles recycle locally after exocytosis without passage through an endosomal intermediate (Barker *et al.*, 1972; Ceccarelli *et al.*, 1973; Zimmermann and Denston, 1977; von Schwarzenfeld, 1979; Henkel and Almers, 1996; Murthy and Stevens, 1998; Ales *et al.*, 1999; Pyle *et al.*, 2000; Stevens and Williams, 2000; Sara *et al.*, 2002; Aravanis *et al.*, 2003; Gandhi and Stevens, 2003). Beyond the involvement of clathrin and its associated proteins such as dynamin and AP180, the mechanisms that mediate and regulate synaptic vesicle recycling are largely unknown (reviewed in Cremona and De Camilli, 1997; Galli and Haucke, 2001; Valtorta *et al.*, 2001; Richmond and Brodie, 2002).

Synaptotagmins are a family of proteins that have been implicated in synaptic vesicle exocytosis, as best characterized for synaptotagmin 1 (Geppert *et al.*, 1994). Synaptotagmins are characterized by an N-terminal transmembrane domain, a central linker and two C-terminal C<sub>2</sub>-domains (Marqueze *et al.*, 2000; Südhof, 2002) that in most synaptotagmins bind Ca<sup>2+</sup>. Synaptotagmin 7 is of particular interest because of its extensive alternative splicing. One of the synaptotagmin 7 splice variants includes a conserved exon with an in-frame stop codon, resulting in a short synaptotagmin 7 variant lacking C<sub>2</sub>-domains (Figure 1A) (Sugita *et al.*, 2001). The C<sub>2</sub>B-domains of synaptotagmins contain a high-affinity binding site for AP-2 and possibly stonin which are involved in clathrin-mediated endocytosis (Zhang *et al.*, 1994; Li *et al.*, 1995; Haucke and De Camilli, 1999; Haucke *et al.*, 2000; Jarousse and Kelly, 2001; Martina *et al.*, 2001), suggesting that synaptotagmins may function in endocytosis in addition to exocytosis. This hypothesis is attractive because it would provide a molecular mechanism to account for the efficient coupling of exo- and endocytosis during neurotransmitter release. Consistent with this hypothesis, vesicles are depleted in *Caenorhabditis elegans* lacking synaptotagmin 1 (Jorgensen *et al.*, 1995), and truncated synaptotagmins similar to the normally occurring short synaptotagmin 7 splice variant are potent inhibitors of clathrin-mediated endocytosis in transfected non-neuronal cells (von Poser *et al.*, 2000). However, little direct evidence for a role of synaptotagmins in synaptic vesicle recycling exists. The presence of short synaptotagmin 7 splice variants in neurons (Sugita *et al.*, 2001) raised the possibility that alternative splicing of synaptotagmin 7 may regulate synaptic vesicle recycling. In the present study, we employed optical and electrophysiological recordings from transfected cultured neurons and electron microscopy to explore this possibility. Our results demonstrate that the short synaptotagmin 7 variant lacking C<sub>2</sub>-domains accelerates endocytic recycling of synaptic vesicles, whereas a regular variant containing C<sub>2</sub>-domains decelerates recycling. These data suggest that two splice variants of a synaptic protein exert opposite actions in regulating vesicle recycling.

## Results

### **Monitoring synaptic vesicle exo- and endocytosis in transfected neurons**

To establish an approach that allows measurements of synaptic vesicle exo- and endocytosis in synapses from transfected neurons, we employed plasmids encoding two splice variants of synaptotagmin 7 that were fused to ECFP (enhanced cyan fluorescent protein; Figure 1A). We used one regular splice variant of synaptotagmin 7 that includes two C<sub>2</sub>-domains (referred to as Svt7A), and a second short

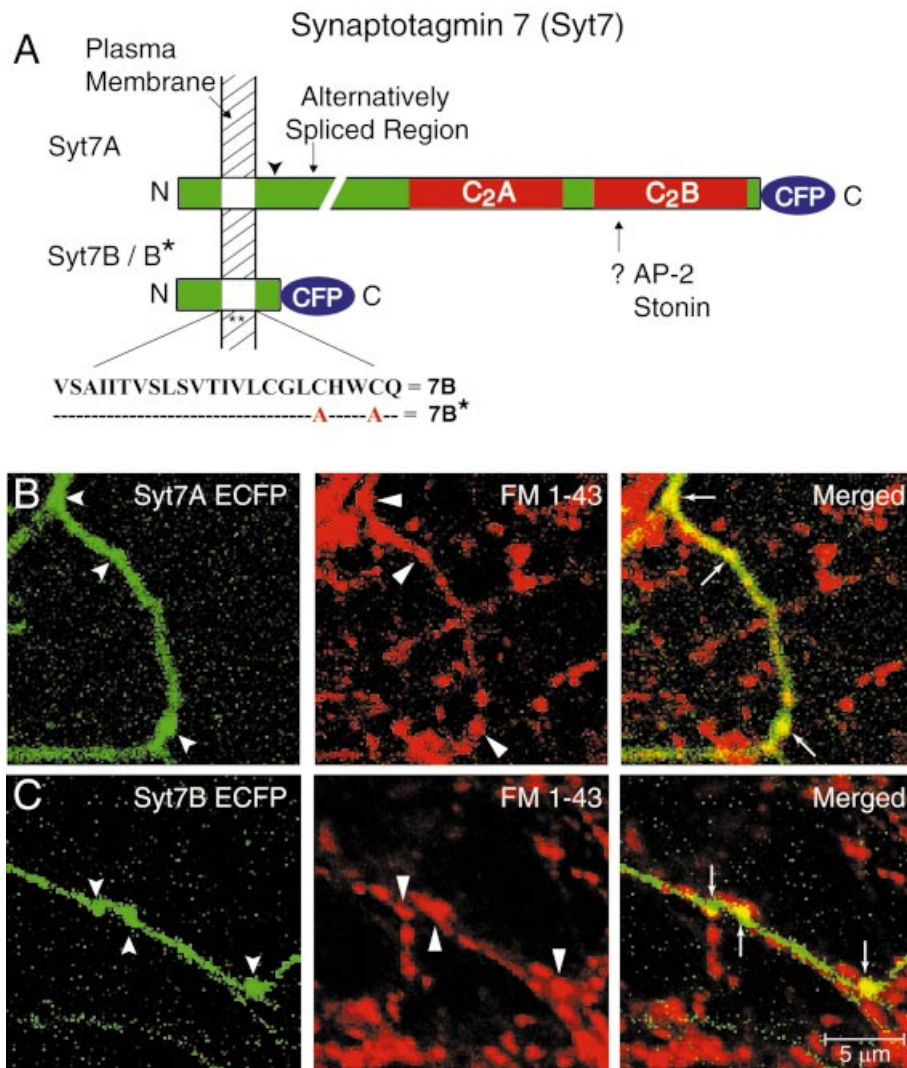


**Fig. 1.** Expression of synaptotagmin 7 splice variants in transfected neurons. (A) Structure of synaptotagmin 7 splice variants (Sugita *et al.*, 2001). All variants share a short N-terminal extracellular sequence and a single transmembrane region but differ in the cytoplasmic sequences where regular synaptotagmin 7 variants contain a variable linker and two C-terminal C<sub>2</sub>-domains, whereas short synaptotagmin 7 variants contain a conserved exon with an in-frame stop codon right after the transmembrane region. The current study employs a regular synaptotagmin 7 variant with a small linker (Syt7A), a short variant with no additional exons (Syt7B), and a mutant short variant in which two cysteine residues in the transmembrane region (see indicated sequence) were substituted for alanine residues to abolish dimerization (Syt7B\*; von Poser *et al.*, 2000). All proteins were fused to enhanced cyan fluorescence protein (CFP). (B and C) Fluorescence images of transfected hippocampal neurons expressing regular (Syt7A; B) or short synaptotagmin 7 (Syt7B; C). Neurons were stained with FM1-43 under stimulation to visualize active presynaptic nerve terminals; merged images of ECFP and FM1-43 fluorescence signals are shown on the right to visualize the presence of transfected synaptotagmin 7 variants in nerve terminals.

splice variant that lacks C<sub>2</sub>-domains (referred to as Syt7B). In addition, we employed a mutant of the short variant in which two cysteine residues in the transmembrane region were substituted by alanine residues (referred to as Syt7B\*). We examined the localization of the ECFP–synaptotagmin 7 fusion proteins in transfected rat hippocampal neurons by fluorescence microscopy, and used staining with FM1-43 to identify presynaptic terminals that contain actively recycling vesicles (Figure 1B and C; Supplementary figure 1 available at *The EMBO Journal* Online). The expressed ECFP–synaptotagmins were present throughout the axons, but enriched in nerve terminals coincident with FM1-43 staining, suggesting that synaptic terminals containing transfected ECFP–synaptotagmin 7 can be readily identified by FM staining and ECFP fluorescence. In order to verify the localization of ECFP–

synaptotagmin 7 fusion proteins, we performed immunocytochemistry using antibodies against ECFP and the presynaptic vesicle protein synaptophysin. This analysis showed significant co-localization of the transfected constructs and synaptophysin (Supplementary figure 2).

#### **The short synaptotagmin 7 splice variant accelerates synaptic vesicle endocytosis**

To test whether synaptotagmin 7 participates in regulating synaptic vesicle endocytosis, we examined the size of synaptic vesicle pools that are labeled with FM1-43 in synapses containing transfected synaptotagmin 7 variants. We first induced exo- and endocytosis of synaptic vesicles by a brief, intense stimulus (field stimulation at 30 Hz for 2 s) that selectively induces exocytosis of the readily releasable vesicle pool (Pyle *et al.*, 2000; Mozhayeva *et al.*,

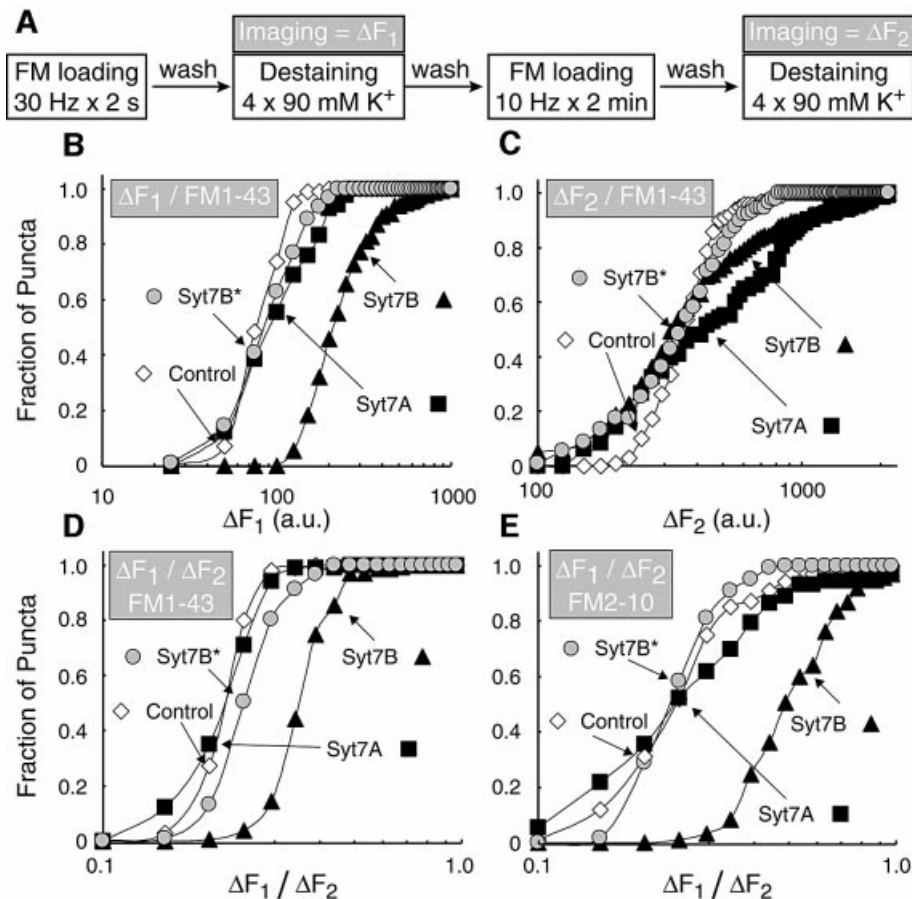


**Fig. 2.** Effect of short and regular synaptotagmin 7 variants on FM dye uptake during stimulation of exocytosis. (A) Experimental design. Neurons were exposed to FM1-43 or FM2-10 during brief electrical stimulation (30 Hz for 2 s), washed for 10 min, and the loss of FM dye from nerve terminals was imaged during repeated stimulations with 90 mM  $K^+$ /2 mM  $Ca^{2+}$  solution to quantify the amount of FM dye that was taken up by actively recycling vesicles during the initial 2 s stimulation ( $\Delta F_1$ ). After a 5 min wash, the same synapses were reloaded with FM1-43 or FM2-10 during prolonged electrical stimulation (10 Hz for 2 min), washed for 10 min, and again imaged during repeated stimulations with 90 mM  $K^+$ /2 mM  $Ca^{2+}$  ( $\Delta F_2$ ). (B and C) Cumulative histograms of the distributions of  $\Delta F_1$  and  $\Delta F_2$ , respectively, in control terminals and in nerve terminals expressing either regular synaptotagmin 7 (Syt7A) or wild-type and mutant short synaptotagmin 7 variants (Syt7B and Syt7B\*, respectively). Data shown are from a representative experiment obtained with FM1-43. (D and E) Cumulative histograms of  $\Delta F_1/\Delta F_2$  ratios from representative experiments obtained with FM1-43 and FM2-10, respectively.

2002). Stimulations were carried out in the presence of FM1-43 which was washed out immediately afterwards, and the size of the recycling vesicle pool was measured by fluorescence imaging as the amount of FM1-43 destaining triggered by four applications of 90 mM  $K^+$  ( $\Delta F_1$ ). Thereafter we stained the same synapses again with FM1-43, but employed a longer stimulus (10 Hz for 2 min) that mobilizes the total pool of recycling vesicles. After the stimulation and subsequent washes, the amount of FM1-43 taken up during the longer stimulus was also imaged as FM destaining caused by  $K^+$  applications ( $\Delta F_2$ ). The second FM1-43 measurements were performed to control for differences between presynaptic terminals in the pools of recycling vesicles and the efficiency of dye labeling. In these experiments, 50–150 nerve terminals were monitored simultaneously on each cover slip, and the data were plotted as cumulative distributions of nerve terminal fluorescence intensities (Figure 2B and C). The medians of such distributions reflect the average size, and their slope the heterogeneity of vesicle pools in the terminals.

We found that the size and heterogeneity of vesicle pools labeled during the brief initial stimulus (Figure 2B) or the longer second stimulus (Figure 2C) were very similar for control terminals and terminals expressing the regular synaptotagmin 7 variant (Syt7A). However, expression of the short synaptotagmin 7 splice variant (Syt7B) caused a 2- to 3-fold increase in the size of the pool labeled by the brief, intense stimulus (Figure 2B), whereas it had no effect on the size of the pool labeled by the longer second stimulus (Figure 2C), as more clearly revealed in plots of the  $\Delta F_1/\Delta F_2$  ratio (Figure 2D). A similar effect was observed when FM1-43 was replaced with another dye, FM2-10, which has faster binding and destaining properties (Figure 2E). The effect by the short synaptotagmin 7 variant was abolished when two cysteine residues in the transmembrane region were mutated to alanine residues (Figure 2D and E). In addition to increasing the  $\Delta F_1/\Delta F_2$  ratio, the short synaptotagmin 7 variant also decreased the slope of the population curve ~3-fold, suggesting that it made the synapses more heterogeneous.

A potential problem of FM staining and destaining experiments is interexperimental variability due, at least in part, to differences between cultures. This variability may be aggravated in transfected neurons because of the nature of the transfections. The actions of the short synaptotagmin 7 variant identified in the present experiments, however, were highly reproducible. The average median  $\Delta F_1/\Delta F_2$  ratio for synapses expressing the short synaptotagmin 7 splice variant was 3-fold higher ( $0.68 \pm 0.13$ ;  $P < 0.01$ ) than that of control synapses ( $0.23 \pm 0.02$ ) or synapses expressing the long synaptotagmin 7 splice variant ( $0.21 \pm 0.03$ ;  $P < 0.01$ ; data are means  $\pm$  standard error of the means (SEMs),  $n = 5-9$  for all comparisons, statistical significance was measured with the two-tailed  $t$ -test). The specificity of the changes induced by the short synaptotagmin 7 variant was confirmed by the finding that nerve terminals containing the mutant short synaptotagmin 7 variant Syt7B\* had a 2-fold lower mean  $\Delta F_1/\Delta F_2$  ratio ( $0.34 \pm 0.07$ ;  $P < 0.05$ ;  $n = 4$ ) than synapses containing the wild-type short synaptotagmin 7 variant. Thus a substitution of only two amino acids in the short synaptotagmin 7 variant (Figure 1A) largely abolished its activity. The decrease in average slope induced by the short synaptotagmin 7 transfection was also highly significant statistically (control =  $7.8 \pm 0.8$ ; Syt7A =  $6.2 \pm 1.6$ ; Syt7B =  $2.7 \pm 0.7$ ;  $P < 0.002$  for control and Syt7A versus Syt7B). Although the number of FM2-10 experiments was too low to allow a statistical analysis, we observed the same difference among transfected synaptotagmin 7 variants as in the FM1-43 experiments, suggesting that the selective effect we observed with the short synaptotagmin 7 splice variant is not a dye-specific phenomenon.

### The short synaptotagmin 7 variant accelerates endocytosis

The data of Figure 2 demonstrate that expression of the short but not a regular synaptotagmin 7 variant induced a major change in the size of the vesicle pool labeled when exocytosis of the readily releasable pool is stimulated. At the same time, the short synaptotagmin 7 variant does not alter the size of the total recycling pool of vesicles. At least two hypotheses could explain the observed effect. (i) The short synaptotagmin 7 variant could increase the number of vesicles that undergo exocytosis and subsequent endocytosis during the  $30 \text{ Hz} \times 2 \text{ s}$  stimulation. Such an increase may involve an enhanced size of the readily releasable pool or an accelerated rate with which vesicles are recruited into the readily releasable pool during stimulation. (ii) Endocytosis of vesicles after exocytosis may be accelerated in synapses overexpressing the short synaptotagmin 7 variant. According to this hypothesis, not all vesicles immediately undergo endocytosis after exocytosis, and an enhanced number of vesicles are labeled during the  $30 \text{ Hz} \times 2 \text{ s}$  stimulation because the short synaptotagmin 7 variant decreases the delay between exo- and endocytosis.

To distinguish between these hypotheses, we first examined the relative size of the readily releasable pool in synapses that express short and long synaptotagmin 7 variants, and the rate with which this pool is emptied upon stimulation. We labeled the total recycling pool of synaptic vesicles with FM2-10 by extensive stimulation

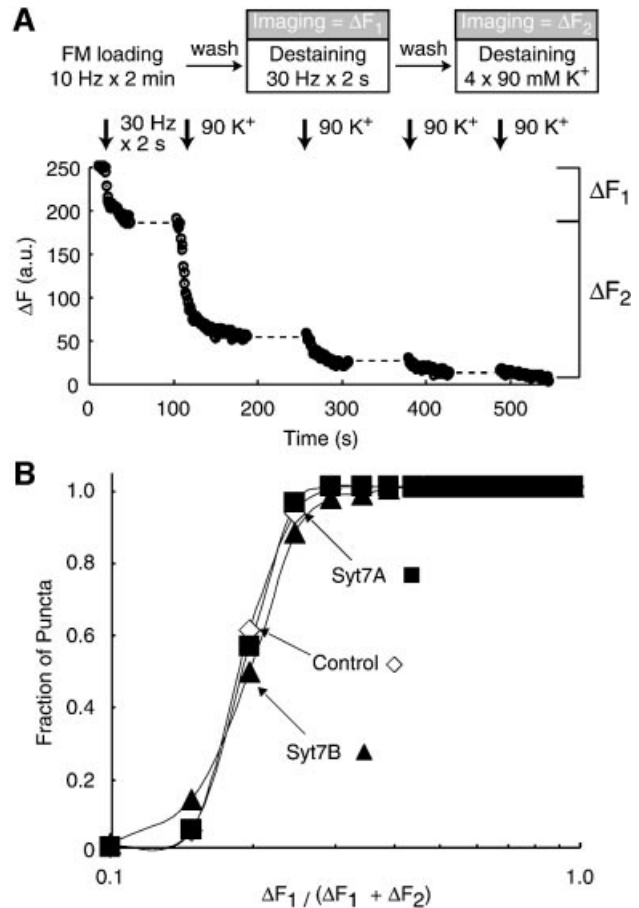


**Fig. 3.** Expression of synaptotagmin 7 variants does not alter the size of the readily releasable pool. (A) Experimental design and sample traces. Nerve terminals were stained with FM2-10 during electrical stimulation at 10 Hz for 2 min, washed for 10 min and FM destaining was imaged while exocytosis of vesicles in the readily releasable pool was induced by 60 stimuli (30 Hz for 2 s;  $\Delta F_1$ ). Afterwards the terminals were washed, and exocytosis of the total pool of recycling vesicles was induced by four applications of 90 mM K<sup>+</sup>/2 mM Ca<sup>2+</sup> ( $\Delta F_2$ ). (B) Cumulative distribution of the ratio of the readily-releasable pool, measured as  $\Delta F_1$ , to the total pool size measured as  $\Delta F_1 + \Delta F_2$  in control synapses and synapses expressing either short and regular synaptotagmin 7 variants. Data shown are from a representative experiment obtained with FM2-10.

(10 Hz for 2 min), washed out the accessible dye, and destained the synapses under imaging with the same  $30 \text{ Hz} \times 2 \text{ s}$  stimulus used to load synapses in the previous protocol (see Figure 2A) to measure the readily releasable pool. Afterwards, we destained the synapses with four applications of 90 mM K<sup>+</sup> to measure the entire recycling pool of vesicles (Figure 3A). We observed no significant difference between control synapses and synapses expressing the short or long synaptotagmin 7 variants in the relative size of the readily releasable pool (Figure 3B) or the rate with which the pool was destained (data not shown). The same results were obtained when we used hypertonic sucrose to measure the readily releasable pool size (Rosenmund and Stevens, 1996) (data not shown).

We next tested whether expression of the short synaptotagmin 7 variant increases the rate of endocytosis. The 'acceleration hypothesis' as described above implies that vesicle endocytosis is usually incomplete when FM1-43 is washed out after the brief  $30 \text{ Hz} \times 2 \text{ s}$  stimulus.

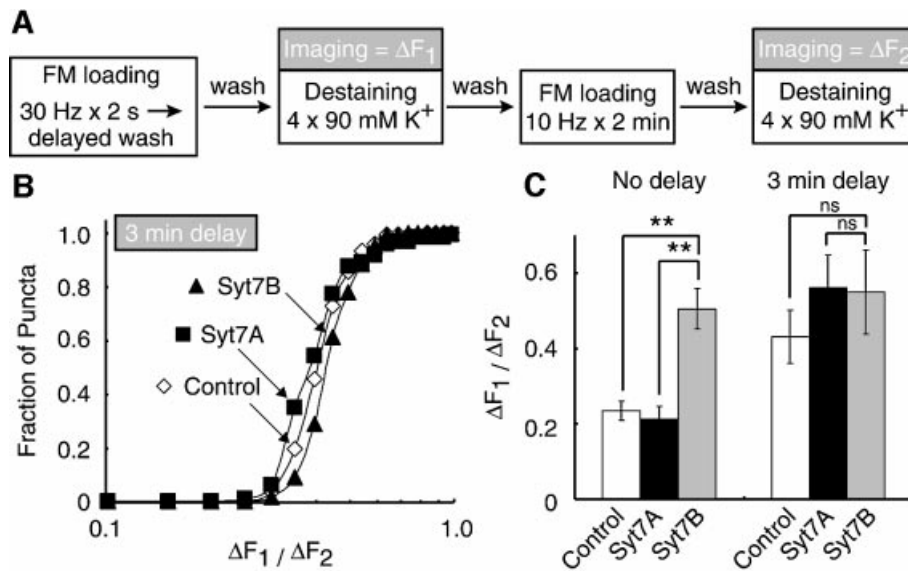


**Fig. 4.** Expression of the short synaptotagmin 7 variant accelerates endocytosis. (A) Experimental design. Nerve terminals were stained and destained as described for Figure 2, except that after the initial electrical stimulation at 10 Hz for 2 min, the washout of the FM dye was delayed for 3 min. (B) Cumulative distribution of the  $\Delta F_1/\Delta F_2$  ratios observed in nerve terminals measured with a 3 min delay of the wash. (C) Bar graphs of the average median  $\Delta F_1/\Delta F_2$  ratios measured without a delay in the wash, or with the 3 min delay (error bars =  $\pm$  SEMs;  $n = 3-6$  coverslips from 2-3 independently transfected cultures; statistical significance was calculated with Student's *t*-test; \*\* $P < 0.01$ ).

Thus we examined whether delaying the washout of FM1-43 after stimulation alters the size of the labeled vesicle pools in control synapses and synapses expressing short or long synaptotagmin 7 variants (Figure 4A). Indeed, a 3 min delay of the wash after the 30 Hz  $\times$  2 s stimulation increased the size of the labeled vesicle pool in control synapses and in synapses expressing regular synaptotagmin 7 (Syt7A), but had no effect on terminals containing the short synaptotagmin 7 variant (Figure 4B and C). As a result, the pool sizes after labeling with a 3 min delay are indistinguishable between control synapses and synapses expressing the short synaptotagmin 7 variant. In contrast, without the delay an  $\sim$ 3-fold difference is observed (Figure 4C), suggesting that expression of the short synaptotagmin 7 variant accelerates the speed of endocytosis.

#### **The long but not short synaptotagmin 7 variant alters FM labeling in response to $K^+$ stimulation**

The data of Figures 2-4 showed that the short synaptotagmin 7 variant most likely accelerates vesicle endocytosis, but did not uncover an effect by the regular synaptotagmin 7 variant. This lack of an effect supports the specificity of the observations made for the short synaptotagmin 7 variant, but does not rule out a role for the regular variant since all of the assays used preferentially detect increases in endocytic recycling, and would have missed a decelerating effect. To test whether a role of the regular synaptotagmin 7 variant in recycling could be detected under stronger stimulation conditions that make it easier to uncover decreases in the rate of recycling, we examined the size of synaptic vesicle pools that are loaded with FM1-43 or FM2-10 during  $K^+$  depolarization which causes maximal exo- and endocytosis (Ryan *et al.*, 1993). We determined the median fluorescence value ( $\Delta F$ ) of control synapses and synapses expressing the short and

regular synaptotagmin 7 variants as described above (Figure 2), and normalized all data for those of control synapses (Figure 5A).

Expression of the regular synaptotagmin 7 variant increased the size of the vesicle pool stained by FM1-43 during  $K^+$  depolarization  $\sim$ 2-fold (Syt7A =  $169 \pm 27\%$  of control;  $P < 0.05$ ;  $n = 11-15$ ), but decreased the pool stained by FM2-10  $>2$ -fold (Syt7A =  $35 \pm 5\%$  of control;  $P < 0.005$ ;  $n = 7-9$ ) (Figure 5B). The short synaptotagmin 7 variant had no significant effect, demonstrating that the changes caused by the regular synaptotagmin 7 variant are not a transfection artifact. Overexpression of synaptotagmin 1, which is very similar in structure to regular synaptotagmin 7, did not show this differential dye uptake (Figure 5C), lending additional support to the specificity of the synaptotagmin 7 effect. The differential effect of the regular synaptotagmin 7 variant on the vesicle pool sizes stained by FM1-43 and FM2-10 suggests that under the conditions of the experiments, the two dyes label at least partly non-overlapping pools. At the neuromuscular junction, FM1-43 becomes trapped during extensive stimulation before endocytosis is completed, while FM2-10 with a faster rate of departitioning is washed out; as a result, the FM1-43 labeled pool is larger and includes vesicles recycling via cisternae that are not detected by FM2-10 (Richards *et al.*, 2000). If this mechanism applied to central synapses, the regular synaptotagmin 7 variant must have shifted synaptic vesicle recycling dramatically from a faster into a slower recycling pathway without changing the overall amount of exocytosis since FM1-43 labeling increases, whereas FM2-10 labeling decreases. The magnitude of the changes suggests that this shift involves the majority of vesicles undergoing exocytosis during the  $K^+$  stimulation.

To test this hypothesis, we examined whether leaving FM2-10 in the solution longer may enable the slowly

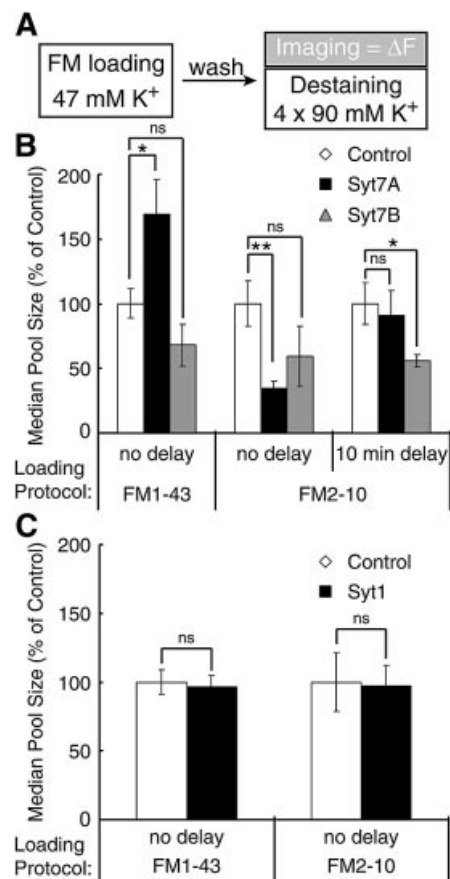


**Fig. 5.** Size of synaptic vesicle pools stained by FM1-43 and FM2-10 during  $K^+$  depolarization. (A) Experimental design. Nerve terminals were stained with FM1-43 or FM2-10 by  $K^+$  depolarization (47 mM  $K^+$ /2 mM  $Ca^{2+}$  for 90 s), washed for 10 min and FM destaining was imaged during repeated  $K^+$  depolarizations to quantify the amount of FM dye taken up in the initial stimulation. (B and C) Bar graphs of the average median  $\Delta F$  values of transfected synapses normalized to non-transfected control synapses under the different loading protocols ( $n = 4$ –15 coverslips from 2–8 independently transfected cultures;  $*P < 0.05$ ;  $**P < 0.005$  student's *t*-test).

recycling pool to take up more FM2-10, comparable to the delay experiments described in Figure 4. After loading FM2-10 into terminals during  $K^+$  depolarization, we incubated synapses for an additional 10 min in FM2-10 in normal extracellular buffer before washing out the dye. The delayed removal of FM2-10 dramatically increased the apparent pool size labeled in synapses expressing the regular synaptotagmin 7 variant, but not in control synapses or synapses expressing the short synaptotagmin 7 variant (Figure 5B).

### Electron microscopy

Among the strongest evidence for two distinct synaptic vesicle recycling pathways are morphological studies in neuromuscular junctions showing that vesicles undergo endocytosis either at the active zone or in the area surrounding the active zone (Koenig and Ikeda, 1996). To determine whether overexpression of synaptotagmin 7 variants have a stimulation-dependent effect on the structure of nerve terminals that could correspond to the

large changes in FM staining observed in the experiments described in Figure 5, we examined transfected neurons—unstimulated or immediately after exposure to 90 mM  $K^+$ —by electron microscopy. Synapses overexpressing the synaptotagmin 7 variants were identified by immunogold labeling with an antibody to the CFP moiety attached to the transfected synaptotagmin 7 (Figure 6). In these electron micrographs, we potentiated the immunogold signal by silver-enhancement; as a result, the immunoreactive material only reports on the general area but not the precise location of the antigen. Nevertheless, consistent with earlier immunoelectron microscopy of endogenous synaptotagmin 7 in brain (Sugita *et al.*, 2001), ECFP–synaptotagmin 7 immunoreactivity was primarily detected close to the plasma membrane or over interior membranes in nerve terminals, whereas the vesicle cluster remained unlabeled (Figure 6).

We then studied the structures of the labeled nerve terminals. We observed no major alterations in unstimulated terminals expressing or lacking synaptotagmin 7 variants. In stimulated nerve terminals, however, overexpression of the regular but not the short synaptotagmin 7 variant induced massive changes: synaptic vesicles were depleted, and large membranous structures—either representing endosomes or plasma membrane cisternae—appeared (Figure 6). Quantitations from two independent experiments confirmed that the short synaptotagmin 7 variant had no large effects on synapse structure, whereas the regular synaptotagmin 7 variant caused a 3- to 4-fold decrease in the density of synaptic vesicles, and 2- to 3-fold increase in the density of non-vesicular membranes in the terminals (Figure 6). These findings, consistent with the FM loading results described in Figure 5, indicate that only the regular form of synaptotagmin 7 induces a shift in synaptic vesicle recycling towards a delayed pathway.

### Overexpression of the regular synaptotagmin 7 variant enhances synaptic depression during repetitive stimulation

Are the changes observed upon synaptotagmin 7 overexpression physiologically significant? Viewed together, our data suggest that the two synaptotagmin 7 splice variants examined here, the short variant lacking  $C_2$ -domains and the regular variant containing  $C_2$ -domains, direct synaptic vesicle recycling into opposite directions: the short variant accelerates recycling, whereas the regular variants promotes a slower, possibly endosomal recycling pathway. However, at least in the case of the regular synaptotagmin 7 variant, we only obtained evidence for a regulatory effect in recycling upon stimulation of exocytosis by strong, unphysiological  $K^+$  depolarizations. More direct would be to measure synaptic transmission, which however is difficult to do in transfected neurons. To achieve this, we optimized the transfection procedure to obtain transfection of at least 10–15% of neurons in our cultures, and then performed recordings during repetitive 10 Hz electrical field stimulation from neurons in regions with a high density of transfected synapses.

When challenged with 10 Hz stimulation, synapses expressing the regular synaptotagmin 7 variant exhibited a significantly faster rate of synaptic depression ( $\tau_{fast} =$  syt7A,  $25.2 \pm 6.4$ ; ECFP,  $82.9 \pm 21.5$ ; syt 1,  $106.3 \pm 24.8$ ; syt7B,  $83.6 \pm 22.1$ ;  $P < 0.03$  for ECFP, syt 1 and

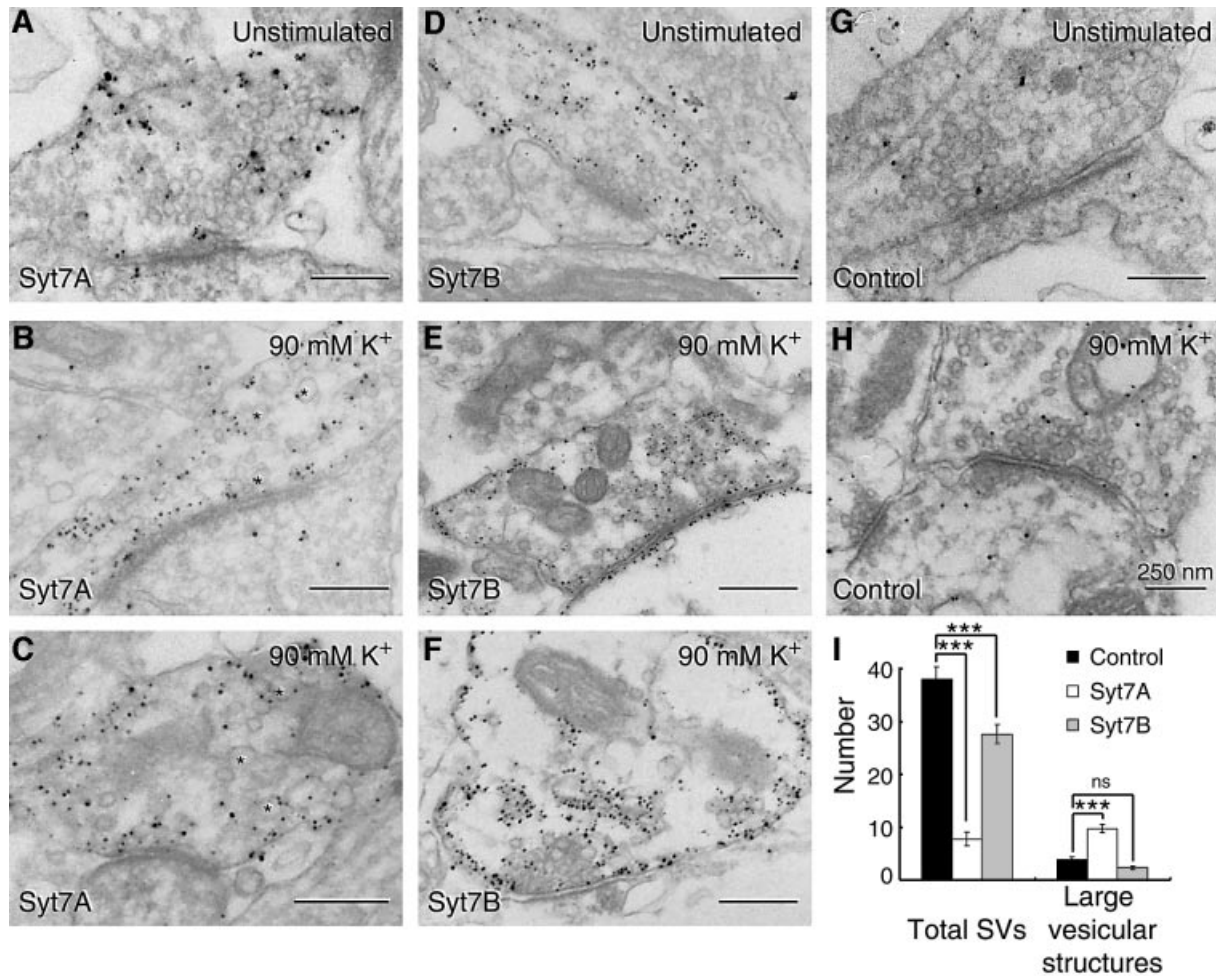


**Fig. 6.** Effect of synaptotagmin 7 overexpression on synaptic ultrastructure. (A–H) Representative immunoelectron micrographs of synapses from transfected neurons examined without stimulation, or after stimulation by K<sup>+</sup> depolarization (90 mM K<sup>+</sup>/2 mM Ca<sup>2+</sup> for 90 s). Neurons were labeled with antibodies to GFP, and signals were amplified by silver enhancement to identify nerve terminals expressing ECFP-tagged synaptotagmin 7 variants. Note that boutons containing regular synaptotagmin 7 (Syt7A) display a depletion of synaptic vesicles and an increase in large vesicular structures (asterisks, diameter >90 nm). (I) Quantification of the number of vesicles and large vesicular structures from electron micrographs. We observed a marked decrease in vesicles (~40 nm) in synapses overexpressing the regular syt7A ( $n = 26$  synapses) compared with non-transfected controls ( $n = 32$  synapses) and syt7B-overexpressing synapses ( $n = 26$  synapses) (\*\* $P < 0.001$ ). In addition, there was an increase in large vesicular structures in syt7A-expressing synapses compared with control and syt7B-transfected synapses (\*\* $P < 0.001$ ).

syt7B versus Syt7A;  $n = 11$ – $12$ ) and a lower steady-state plateau than synapses expressing either ECFP or syt 1 as transfection controls (syt7A,  $0.12 \pm 0.02$ ; ECFP,  $0.24 \pm 0.04$ ; syt 1,  $0.21 \pm 0.04$ ;  $P < 0.03$ ) (Figure 7A and B). In contrast, neurons from cultures transfected with the short synaptotagmin 7 variant displayed a slightly elevated level of sustained release ( $0.27 \pm 0.04$ ). The starting amplitudes of synaptic responses, as measured in multiple independent experiments, were also similar for all the different conditions studied (Syt7A =  $-1214 \pm 162$  pA; Syt7B =  $-1345 \pm 230$  pA; ECFP =  $-1092 \pm 174$  pA; Syt 1 =  $-1158 \pm 171$  pA;  $n = 11$ – $12$ ). The similar size of synaptic responses after expression of the short or regular synaptotagmin 7 variant indicates that these variants do not cause differential effects on the number of synapses or synaptic release probability. Thus the distinct effects of the two synaptotagmin 7 variants on the rate of use-dependent depression during the 10 Hz stimulation (Figure 7) must be related to the endocytosis and recycling of synaptic vesicles.

## Discussion

Nerve terminals contain at least two different pools of synaptic vesicles, a readily releasable pool and a reluctant or reserve pool (Neher, 1998). When a nerve terminal is stimulated, readily releasable vesicles undergo exocytosis first, while reserve vesicles are recruited for exocytosis when the readily releasable pool has been exhausted. After exocytosis, the two pools appear to be re-filled via at least two recycling pathways: a fast pathway that preferentially refills the readily releasable pool, and a slower pathway that preferentially directs vesicles into the reserve pool (Richards *et al.*, 2000; Li and Murthy, 2001). In spite of extensive physiological characterization, the molecular mechanisms involved in the release and recycling of vesicle pools remain unclear. In the present study, we show that two splice variants of synaptotagmin 7 differentially affect synaptic vesicle recycling. Our results build on previous studies demonstrating that in non-neuronal cells, truncated synaptotagmin 7 inhibits clathrin-mediated

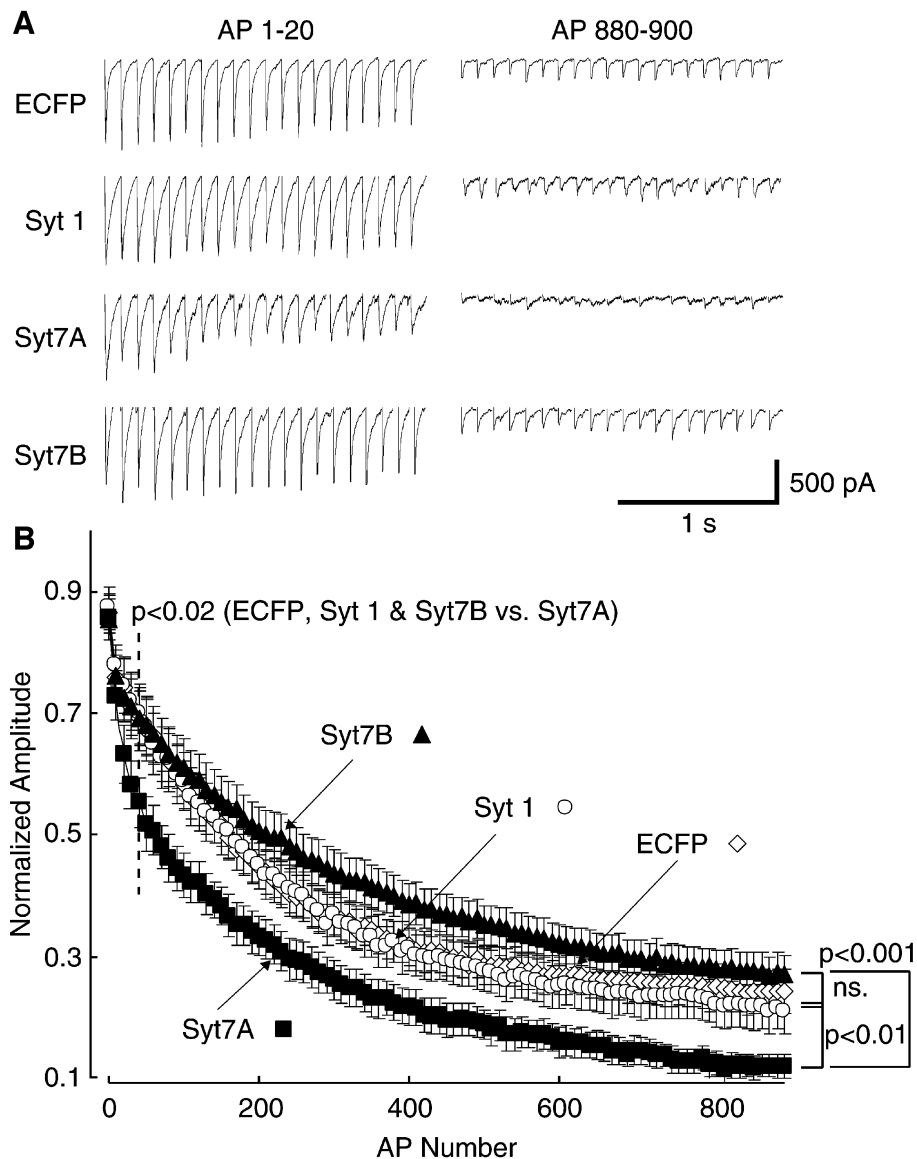


**Fig. 7.** Effect of synaptotagmin 7 overexpression on synaptic responses recorded electrophysiologically. **(A)** Representative whole-cell recordings in neurons from cultures transfected at high efficiency with regular synaptotagmin 7 (Syt7A), short synaptotagmin 7 (Syt7B) and two control proteins, synaptotagmin 1 (syt 1) and ECFP alone. Recordings were made during 10 Hz stimulation from high-density cultures with each signal resulting from multiple synapses per neuron; only the first and last 20 responses during a total of 900 stimuli are shown. **(B)** Average normalized response amplitudes from cells stimulated at 10 Hz by field electrodes. Each point represents the average of 10 consecutive responses. Syt7B overexpression results in a higher steady-state plateau of response amplitudes. In contrast, syt7A overexpression results in faster depression of the initial responses ( $P < 0.02$ ;  $n = 12$ ) as well as a lower response amplitude at steady-state compared with both controls ( $P < 0.03$ ;  $n = 11$ –12) and Syt7B ( $P < 0.001$ ;  $n = 11$ ) overexpression.

endocytosis (von Poser *et al.*, 2000), and that in neuronal cells, a splice variant of synaptotagmin 7 encoding a truncated form is normally expressed (Sugita *et al.*, 2001). Our data are consistent with a simplistic model whereby a ‘checkpoint’ after exocytosis controls the recycling pathway of a vesicle, and the checkpoint is manned by alternatively spliced variants of synaptotagmin 7.

In our experiments, we have made two principal observations. (i) The short synaptotagmin 7 variant accelerates endocytosis during brief stimuli that preferentially release vesicles of the readily releasable pool. (ii) In contrast, the regular C<sub>2</sub>-domain containing synaptotagmin 7 variant directs synaptic vesicles into a slow recycling pathway. The first conclusion is based on the

following evidence. (i) The short synaptotagmin 7 variant increased FM labeling of recycling vesicles during brief, intense stimuli (Figure 2). (ii) The increase in FM labeling under these conditions was abolished when the FM dye was not washed out immediately after the stimulation (Figure 4). (iii) The short synaptotagmin 7 variant had no significant effect on other parameters, including the structure of nerve terminals as visualized by electron microscopy (Figure 6), the rate of exocytosis (data not shown), the relative size of the readily releasable pool (Figure 3), or the amount of release that was stimulated by a single action potential (Figure 7). Conversely, the second conclusion—that the regular synaptotagmin 7 variant redirects recycling vesicles into a slow recycling path-



way—is based on the following evidence. (i) Overexpression of the regular synaptotagmin 7 variant caused a large shift in pool sizes of vesicles labeled with FM1-43 and FM2-10 when terminals were stimulated maximally by K<sup>+</sup> depolarization (Figure 5). No such shift was observed for less extensive labeling conditions, e.g. application of 1200 action potentials at 10 Hz for 2 min (Figure 2). (ii) Stimulation of nerve terminals containing overexpressed regular synaptotagmin 7 variant caused depletion of synaptic vesicles and generation of large endosomal or cisternal structures (Figure 6). (iii) The regular synaptotagmin 7 variant did not alter the amount of initial release as measured electrophysiologically, but induced faster synaptic depression during 10 Hz stimulation consistent with delayed recycling (Figure 7). (iv) In all other parameters measured, especially in the size of the readily releasable pool (Figure 3), the kinetics of release when stimulated under submaximal conditions (data not shown), and the amount of FM labeled vesicles under submaximal stimulation conditions (Figure 2), nerve terminals containing transfected regular synaptotagmin 7 variant were undistinguishable from controls. This indicates that consistent with the electron micrographs of resting nerve terminals containing overexpressed synaptotagmin 7 (Figure 6), synaptotagmin 7 did not alter the structure of resting nerve terminals.

Regulation of synaptic vesicle recycling by alternative splicing of synaptotagmin 7 may participate in shaping synaptic transmission during high-frequency trains of action potentials, as are commonly observed in central neurons (Connors and Amitai, 1997; Brumberg *et al.*, 2000). A strength of our findings lies in the fact that the two splice variants of synaptotagmin 7 tested exerted distinct effects in every assay used. The two variants thus control for each other, and exclude transfection/overexpression artifacts. In particular, the observed changes are not an effect created by ECFP overexpression since all proteins contained the same ECFP moieties in spite of having distinct actions. The finding that the action of the shorter splice variant can be abolished by point mutations in the transmembrane region which interfere with palmitoylation, and that synaptotagmin 1 does not mimic the regular length splice variant further argues against a simple overexpression artifact. However, we cannot exclude the possibility that the overexpressed proteins, in their opposing effects, do not mimic the actions of the endogenous proteins; only knockouts and/or knockins will resolve this possibility unambiguously. Another caveat is that the implications of our results are limited to endocytosis and pools sizes, and do not allow conclusions about the possible role of synaptotagmin 7 variants in the timing or rate of exocytosis.

What is the mechanism by which the two synaptotagmin 7 variants direct vesicles into distinct recycling pathways? Mutation of two cysteine residues in the transmembrane region (Figure 1A) abolishes the effect of the short variant (see Figure 2). These cysteines were shown to be palmitoylated and to mediate synaptotagmin 7 dimerization (von Poser *et al.*, 2000), suggesting that synaptotagmin 7 dimerization may be essential for its action. The C<sub>2</sub>-domains of synaptotagmin 7 bind to all negatively charged phospholipids (Li *et al.*, 1995; Shin *et al.*, 2002), preferentially phospholipids with multiple

negative charges such as phosphatidylinositol-bis-phosphate, and could thus interact with this lipid that has been shown to function in endocytosis (Cremona *et al.*, 1999; Ford *et al.*, 2001). The C<sub>2</sub>B-domain binds with high affinity to the endocytic adaptor protein AP-2 (Li *et al.*, 1995) and may also interact with stonins as shown for synaptotagmin 1 (Martina *et al.*, 2001; Walther *et al.*, 2001), although this has not yet been tested. Viewed together, these findings are consistent with the hypothesis that interactions of the synaptotagmin 7 C<sub>2</sub>-domains with molecules involved in endocytosis (PIP<sub>2</sub>, AP-2 and possibly stonin) promote clathrin-coated endocytosis only when the C<sub>2</sub>-domains are attached to a dimer of synaptotagmin 7 variants in which both protein molecules contain C<sub>2</sub>-domains. This hypothesis is supported by previous studies demonstrating that a truncated synaptotagmin 7 variant which is similar to the normally expressed short splice variant, when overexpressed in fibroblasts, inhibits the recruitment of clathrin coats to the plasma membrane (von Poser *et al.*, 2000). This hypothesis would explain the differential effects of short and regular synaptotagmin 7 variants on endocytic recycling of synaptic vesicles: overexpression of the short synaptotagmin 7 variant would titrate out endogenous full-length synaptotagmin 7, and thereby downregulate clathrin-dependent endocytosis, whereas overexpression of the regular synaptotagmin 7 variant would dilute out endogenous short synaptotagmin 7 variant and thereby promote clathrin-coated endocytosis. A balance between splice variants is attractive as a regulatory mechanism because it allows fine-tuning, but this is at present only a working hypothesis which requires additional evidence.

## Materials and methods

### Cell culture

Dissociated hippocampal cultures were prepared from 1- to 2-day-old Sprague–Dawley rats as described (Kavalali *et al.*, 1999), and transfected after 6 days *in vitro* using a calcium phosphate transfection protocol with pCMV5-vectors containing CFP fusion proteins of full-length synaptotagmin 7 (syt7A), truncated synaptotagmin 7 (syt7B) or truncated synaptotagmin 7 with C to A mutations at residues 38 and 41 in the transmembrane region of the protein (syt7B\*) (Figure 1). The constructs were made from cDNA clones as described (Sugita *et al.*, 2001). Cells were imaged at day 10–11 *in vitro* 4–5 days after transfections.

### Fluorescence imaging

Synaptic boutons were loaded with either FM2-10 (400 μM) or FM1-43 (8 μM) (Molecular Probes, Eugene, OR) using either electric field stimulation in the presence of 4 mM K<sup>+</sup>, 2 mM Ca<sup>2+</sup> solution or 90 s incubation in hyperkalemic solution 47 mM K<sup>+</sup>/2 mM Ca<sup>2+</sup>. Modified Tyrode solution containing (in mM) 150 NaCl, 4 KCl, 2 MgCl<sub>2</sub>, 10 glucose, 10 HEPES and 2 CaCl<sub>2</sub> (pH 7.4, ~310 mOsm) was used in all experiments. Hypertonic solution was prepared by addition of 500 mM sucrose to the modified Tyrode solution. The 90 mM K<sup>+</sup> solutions contained equimolar substitution of KCl for NaCl. Field stimulation was applied through parallel platinum electrodes immersed into the perfusion chamber delivering 25 mA–1 ms pulses. All staining protocols were performed with 10 μM CNQX and 50 μM AP-5 to prevent recurrent activity. Images were taken after 10 min washes in dye-free solution in nominal Ca<sup>2+</sup> to minimize spontaneous dye loss. Destaining of hippocampal terminals with hypertonic/high-potassium challenge was achieved by direct perfusion of solutions onto the field of interest by gravity (2 ml/min). Images were obtained by a cooled-intensified digital CCD camera (Roper Scientific, Trenton, NJ) during illumination (1 Hz, 60 ms) at 480 ± 20 nm (505 DCLP, 535 ± 25 BP) via an optical switch (Sutter Instruments, Novato, CA). Images were acquired and analyzed

using Axon Imaging Workbench Software (Axon Instruments, Union City, CA).

### Electrophysiology

Whole-cell recordings from pyramidal cells were acquired with an Axopatch 200B amplifier and Clampex 8.0 software (Axon Instruments, Union City, CA). Recordings were filtered at 2 kHz and sampled at 200  $\mu$ s. Pipette internal solution included (in mM): 115 Cs-MeSO<sub>3</sub>, 10 CsCl, 5 NaCl, 10 HEPES, 0.6 EGTA, 20 TEACl, 4 Mg<sup>2+</sup>-ATP, 0.3 Na<sub>2</sub>GTP, 10 QX-314 (pH 7.35, 300 mOsm).

### Electron microscopy

Transfected cells were stimulated with 90 mM K<sup>+</sup> solution or control buffer for 90 s, fixed in 1% glutaraldehyde, 2% paraformaldehyde in PBS (pH 7.4), and examined by immunoelectron microscopy using a rabbit antibody to GFP essentially as described (Sugita *et al.*, 2001).

### Immunostaining

For immunocytochemistry, neurons were fixed with 4% formaldehyde/PBS and were permeabilized in 0.4% saponin. Primary antibodies used in this study were anti-synaptophysin monoclonal (1:1000) (to identify presynaptic terminals), anti-GFP polyclonal (1:1000) (to identify transfected proteins). Secondary antibodies were Alexa 488-conjugated goat anti-rabbit and Alexa 568-conjugated goat anti-mouse (Molecular Probes). Fluorescence micrographs were taken using a Leica TCS SP2 Laser Scanning Spectral Confocal microscope.

### Miscellaneous

All error bars denote SEM; all *n* values correspond to individual coverslips unless mentioned otherwise; all statistical assessments were performed with the two-tailed *t*-test.

### Supplementary data

Supplementary data are available at *The EMBO Journal* Online.

## Acknowledgements

We would like to thank Y.Sara, M.Mozhayeva, F.Deak, L.Monteggia and K.Huber for advice, M.Mahgoub for technical assistance. T.V. is supported by the Medical Scientist Training Program. E.T.K is the Effie Marie Cain Endowed Scholar in Biomedical Research at the University of Texas Southwestern Medical Center.

## References

Ales,E., Tabares,L., Poyato,J.M., Valero,V., Lindau,M. and Alvarez de Toledo,G. (1999) High calcium concentrations shift the mode of exocytosis to the kiss-and-run mechanism. *Nat. Cell Biol.*, **1**, 40–44.

Aravanis,A.M., Pyle,J.L. and Tsien,R.W. (2003) Single synaptic vesicles fusing transiently and successively without loss of identity. *Nature*, **423**, 643–647.

Barker,L.A., Dowdall,M.J. and Whittaker,V.P. (1972) Choline metabolism in the cerebral cortex of guinea pigs. Stable-bound acetylcholine. *Biochem. J.*, **130**, 1063–1075.

Betz,W.J. and Bewick,G.S. (1993) Optical monitoring of transmitter release and synaptic vesicle recycling at the frog neuromuscular junction. *J. Physiol.*, **460**, 287–309.

Brumberg,J.C., Nowak,L.G. and McCormick,D.A. (2000) Ionic mechanisms underlying repetitive high-frequency burst firing in supragranular cortical neurons. *J. Neurosci.*, **20**, 4829–4843.

Ceccarelli,B., Hurlbut,W.P. and Mauro,A. (1973) Turnover of transmitter and synaptic vesicles at the frog neuromuscular junction. *J. Cell Biol.*, **57**, 499–524.

Connors,B.W. and Amitai,Y. (1997) Making waves in the neocortex. *Neuron*, **18**, 347–349.

Cremona,O. and De Camilli,P. (1997) Synaptic vesicle endocytosis. *Curr. Opin. Neurobiol.*, **7**, 323–330.

Cremona,O. *et al.* (1999) Essential role of phosphoinositide metabolism in synaptic vesicle recycling. *Cell*, **99**, 179–188.

Ford,M.G., Pearce,B.M., Higgins,M.K., Vallis,Y., Owen,D.J., Gibson,A., Hopkins,C.R., Evans,P.R. and McMahon,H.T. (2001) Simultaneous binding of PtdIns(4,5)P<sub>2</sub> and clathrin by AP180 in the nucleation of clathrin lattices on membranes. *Science*, **291**, 1051–1055.

Galli,T. and Haucke,V. (2001) Cycling of synaptic vesicles: how far? How fast! *Sci. STKE*, **2001**, RE1.

Gandhi,S.P. and Stevens,C.F. (2003) Three modes of synaptic vesicular recycling revealed by single-vesicle imaging. *Nature*, **423**, 607–613.

Geppert,M., Goda,Y., Hammer,R.E., Li,C., Rosahl,T.W., Stevens,C.F. and Sudhof,T.C. (1994) Synaptotagmin I: a major Ca<sup>2+</sup> sensor for transmitter release at a central synapse. *Cell*, **79**, 717–727.

Haucke,V. and De Camilli,P. (1999) AP-2 recruitment to synaptotagmin stimulated by tyrosine-based endocytic motifs. *Science*, **285**, 1268–1271.

Haucke,V., Wenk,M.R., Chapman,E.R., Farsad,K. and De Camilli,P. (2000) Dual interaction of synaptotagmin with  $\mu$ 2- and  $\alpha$ -adaptorin facilitates clathrin-coated pit nucleation. *EMBO J.*, **19**, 6011–6019.

Henkel,A.W. and Almers,W. (1996) Fast steps in exocytosis and endocytosis studied by capacitance measurements in endocrine cells. *Curr. Opin. Neurobiol.*, **6**, 350–357.

Heuser,J.E. and Reese,T.S. (1973) Evidence for recycling of synaptic vesicle membrane during transmitter release at the frog neuromuscular junction. *J. Cell Biol.*, **57**, 315–344.

Jarousse,N. and Kelly,R.B. (2001) The AP2 binding site of synaptotagmin I is not an internalization signal but a regulator of endocytosis. *J. Cell Biol.*, **154**, 857–866.

Jorgensen,E.M., Hartwig,E., Schuske,K., Nonet,M.L., Jin,Y. and Horvitz,H.R. (1995) Defective recycling of synaptic vesicles in synaptotagmin mutants of *Caenorhabditis elegans*. *Nature*, **378**, 196–199.

Kavalali,E.T., Klingauf,J. and Tsien,R.W. (1999) Activity-dependent regulation of synaptic clustering in a hippocampal culture system. *Proc. Natl Acad. Sci. USA*, **96**, 12893–12900.

Koenig,J.H. and Ikeda,K. (1996) Synaptic vesicles have two distinct recycling pathways. *J. Cell Biol.*, **135**, 797–808.

Li,C., Ullrich,B., Zhang,J.Z., Anderson,R.G., Brose,N. and Sudhof,T.C. (1995) Ca(2+)-dependent and -independent activities of neural and non-neural synaptotagmins. *Nature*, **375**, 594–599.

Li,Z. and Murthy,V.N. (2001) Visualizing postendocytic traffic of synaptic vesicles at hippocampal synapses. *Neuron*, **31**, 593–605.

Liu,G. and Tsien,R.W. (1995) Properties of synaptic transmission at single hippocampal synaptic boutons. *Nature*, **375**, 404–408.

Marqueze,B., Berton,F. and Seagar,M. (2000) Synaptotagmins in membrane traffic: which vesicles do the tagmins tag? *Biochimie*, **82**, 409–420.

Martina,J.A., Bonangelino,C.J., Aguilar,R.C. and Bonifacino,J.S. (2001) Stonin 2: an adaptor-like protein that interacts with components of the endocytic machinery. *J. Cell Biol.*, **153**, 1111–1120.

Mozhayeva,M.G., Sara,Y., Liu,X. and Kavalali,E.T. (2002) Development of vesicle pools during maturation of hippocampal synapses. *J. Neurosci.*, **22**, 654–665.

Murthy,V.N. and Stevens,C.F. (1998) Synaptic vesicles retain their identity through the endocytic cycle. *Nature*, **392**, 497–501.

Neher,E. (1998) Vesicle pools and Ca<sup>2+</sup> microdomains: new tools for understanding their roles in neurotransmitter release. *Neuron*, **20**, 389–399.

Pyle,J.L., Kavalali,E.T., Piedras-Renteria,E.S. and Tsien,R.W. (2000) Rapid reuse of readily releasable pool vesicles at hippocampal synapses. *Neuron*, **28**, 221–231.

Richards,D.A., Guatimosim,C. and Betz,W.J. (2000) Two endocytic recycling routes selectively fill two vesicle pools in frog motor nerve terminals. *Neuron*, **27**, 551–559.

Richmond,J.E. and Brodie,K.S. (2002) The synaptic vesicle cycle: exocytosis and endocytosis in *Drosophila* and *C. elegans*. *Curr. Opin. Neurobiol.*, **12**, 499–507.

Rosenmund,C. and Stevens,C.F. (1996) Definition of the readily releasable pool of vesicles at hippocampal synapses. *Neuron*, **16**, 1197–1207.

Ryan,T.A., Reuter,H., Wendland,B., Schweizer,F.E., Tsien,R.W. and Smith,S.J. (1993) The kinetics of synaptic vesicle recycling measured at single presynaptic boutons. *Neuron*, **11**, 713–724.

Sara,Y., Mozhayeva,M.G., Liu,X. and Kavalali,E.T. (2002) Fast vesicle recycling supports neurotransmission during sustained stimulation at hippocampal synapses. *J. Neurosci.*, **22**, 1608–1617.

Shin,O.H., Rizo,J. and Sudhof,T.C. (2002) Synaptotagmin function in dense core vesicle exocytosis studied in cracked PC12 cells. *Nat. Neurosci.*, **5**, 649–656.

Stevens,C.F. and Williams,J.H. (2000) ‘Kiss and run’ exocytosis at hippocampal synapses. *Proc. Natl Acad. Sci. USA*, **97**, 12828–12833.

Sudhof,T.C. (2002) Synaptotagmins: why so many? *J. Biol. Chem.*, **277**, 7629–7632.

Sugita,S., Han,W., Butz,S., Liu,X., Fernandez-Chacon,R., Lao,Y. and

- Sudhof,T.C. (2001) Synaptotagmin VII as a plasma membrane  $Ca^{2+}$  sensor in exocytosis. *Neuron*, **30**, 459–473.
- Takei,K., Mundigl,O., Daniell,L. and De Camilli,P. (1996) The synaptic vesicle cycle: a single vesicle budding step involving clathrin and dynamin. *J. Cell Biol.*, **133**, 1237–1250.
- Valtorta,F., Meldolesi,J. and Fesce,R. (2001) Synaptic vesicles: is kissing a matter of competence? *Trends Cell Biol.*, **11**, 324–328.
- von Poser,C., Zhang,J.Z., Mineo,C., Ding,W., Ying,Y., Sudhof,T.C. and Anderson,R.G. (2000) Synaptotagmin regulation of coated pit assembly. *J. Biol. Chem.*, **275**, 30916–30924.
- von Schwarzenfeld,I. (1979) Origin of transmitters released by electrical stimulation from a small metabolically very active vesicular pool of cholinergic synapses in guinea-pig cerebral cortex. *Neuroscience*, **4**, 477–493.
- Walther,K., Krauss,M., Diril,M.K., Lemke,S., Ricotta,D., Honing,S., Kaiser,S. and Haucke,V. (2001) Human stoned B interacts with AP-2 and synaptotagmin and facilitates clathrin-coated vesicle uncoating. *EMBO Rep.*, **2**, 634–640.
- Zhang,J.Z., Davletov,B.A., Sudhof,T.C. and Anderson,R.G. (1994) Synaptotagmin I is a high affinity receptor for clathrin AP-2: implications for membrane recycling. *Cell*, **78**, 751–760.
- Zimmermann,H. and Denston,C.R. (1977) Separation of synaptic vesicles of different functional states from the cholinergic synapses of the Torpedo electric organ. *Neuroscience*, **2**, 715–730.

*Received May 30, 2003; revised August 4, 2003;  
accepted August 15, 2003*